



Shahid Chamran
University of Ahvaz

Journal of Applied and Computational Mechanics



Research Paper

Influence of Thermophysical Features on MHD Squeezed Flow of Dissipative Casson Fluid with Chemical and Radiative Effects

Mojeed T. Akolade¹, Adeshina T. Adeosun², John O. Olabode³

¹ Department of Mathematics, Faculty of physical sciences, University of Ilorin, Ilorin, Nigeria, Email: 17-68ev006pg@students.unilorin.edu.ng

² Department of Mathematics, Faculty of physical sciences, University of Ilorin, Ilorin, Nigeria, Email: shiteq99@gmail.com

³ Department of Mathematics, Faculty of physical sciences, University of Ilorin, Ilorin, Nigeria, Email: johnoluwasina34@gmail.com

Received September 06 2020; Revised November 03 2020; Accepted for publication November 06 2020.

Corresponding author: M.T. Akolade (17-68ev006pg@students.unilorin.edu.ng)

© 2021 Published by Shahid Chamran University of Ahvaz

Abstract. Theoretical investigation of variable mass diffusivity, thermal conductivity, and viscosity on unsteady squeezed flow of dissipative Casson fluid is presented. Physically, for any effective heat and mass transfer process, a proper account of thermophysical properties in such a system is required to attain the desired production output. The magnetized free convective flow of unsteady Casson fluid encompassing Joule dissipation, radiation, and chemical reactive influence is induced as a result of squeezing property. The governing model assisting the magnetized flow is formulated and transformed via an appropriate similarity transformation. The resulting set of ordinary differential equations is solved numerically using Chebyshev based Collocation Approach (CCA). However, variable viscosity, thermal conductivity, and mass diffusivity effects are seen to diminish the fluid flow velocities, temperature, and concentration respectively along with the lower plate. Heat and mass transfer coefficient, skin friction downsized to an increasing value of variable thermal and mass diffusivity parameters while variable viscosity pronounces the skin friction coefficient. Furthermore, the present analysis is applicable in polymer processing, such as injection molding, extrusion, thermoforming among others.

Keywords: Casson fluid; Chebyshev Collocation Method, Squeezing flow, MHD, Thermophysical properties.

1. Introduction

The study of the deformation process between plates or objects was first investigated by Stefan [1], the process that describes the external and internal factors such as viscoelasticity and temperature effects, the outward droplet of materials, etc., generally referred to as Squeezing flow. The biological and industrial applications include, the flows through nasogastric tubes, syringes, synthetics transportation, and exhibition of squeezing movement such as to-and-fros locomotion in pistons, clutching flow, electric motors, automobile engines, bioengineering, squeezed films in power transmission, and many more ([2],[3]). The temperature common-cause effect in the heat and mass transfer process known as thermophysical variation is best explained as the required temperature variation within the flow system. Due to low sensitivity to temperature changes, it is imperative to examine the temperature variation effect in MHD squeezing flow of dissipative Casson fluid considering its application occurrence both in industries and nature.

With these numerous practical and industrial applications, the dynamic of squeezing flow in different geometries and base fluid is pronounced. Series of literature on the modeling of squeeze flow include Mustafa et al. [2] on heat and mass transfer of Newtonian fluid flow, Ahmed et al. [4], Khan et al. [3], Qayyum et al. [5], Naduvanamani and Shankar [6] on Casson rheology through a parallel plate with distinct flow assumptions. Singh et al. [7] assumed water as a base fluid with the presence of nanoparticles and velocity slip, Ghadikolaei et al. [8] on Eyring-Powell fluid, Hussain et al. [9] on Walters'B viscoelastic fluid. Ahmad et al. [10] present the slip analysis of squeezing flow in a doubly stratified fluid. Ahmad et al [11] gave the squeezing flow analysis of convectively heated fluid in a porous medium with activation energy and binary chemical reaction. Hosseinzadeh et al. [12] accounted for the MHD squeezing nanofluid flow problem by employing a series of semi-analytical methods. Local linearization (Spectral) technique was employed by Thumma and Magagula [13] to approximate the solution of squeezing flow between two parallel Riga plates. They reported that a rise in squeezing property improved both momentum and temperature profiles.

Recently, Salehi et al. [14] presented the analysis of Hydrothermal MHD squeezing mixture fluid suspended by hybrid nanoparticles. Electroviscous study of squeezing flow of thin electrolyte solution films by Zhao et al. [15] reveals that the velocity profile is enhanced to a higher value of dissipative hydrodynamic interaction force. Khan et al. [16] modeled the Squeezing flow of nanofluids with mixed convection effects in the three-dimensional region. They reported that a significant influence of nanofluids on the velocity profile is perceived to an enormous value of mixed convection parameter. While Ahmad et al. [17] introduced the melting phenomenon on squeezing flow of chemically reacting Jeffrey fluid past infinite parallel plates. In their



study energy and momentum of Jeffrey fluid is appreciated to a higher magnitude of melting parameter while energy distribution decays for dominant of thermal radiation parameter. Qayyum et al. [18] analyzed the magnetic field influence in three dimensional nanofluid motion. Their analysis reveals the significant impact of squeezing number on the flow motion. Korczyk et al. [19] account the droplet formation in the microfluidic channel while predicting the droplet characterizes and size transitions from leaking-squeezing-jetting in microfluidic channels, and Perturbation-Iteration Algorithm (PIA), a numerical approach was implemented by Al-Saif and Harfash [20] on the squeezing flow encompassing the dissipative effect rather than well know semi-analytical methods.

Without loss of generality, the fluid thermophysical features are most sensitive to temperature rise, hence, these properties are known to vary significantly when subjected to temperature changes. For instance, a corresponding rise in temperature and heat generated by the internal friction of a lubricating fluid affects the fluid viscosity, while a rise in temperature appreciates the local increase in transport mechanism by depreciating the viscosity across the momentum boundary layer (Animasaun [21]). The higher the temperature the more frequent the spontaneous fluctuations in blood flow (Barcroft and Edholm [22]). On these notes, the assumptions of constant fluid physical properties failed. However, researchers attention drawn into the thermophysical modeling in different fluid rheology and physical geometry was analyzed, among which Khan et al. [23] and Basha et al. [24] presented their thermophysical investigation on Williamson Nanofluid, Waqas et al. [25] on Carreau fluid, Abdul Wahab et al. [26] on Eyring-Powell fluid with Double Stratification effects, Omowaye and Animasaun [27] on upper Maxwell converted fluid, and series of studies on Casson fluid includes Mondal et al. [28], Salahuddin et al. [29], Idowu and Falodun [30] with Soret-Dufour influence, Gbadeyan et al. [31] with velocity slip and convective heating effect. Hazarika et al. [32] presented their variable thermophysical study past a cone geometry. Lu et al. [33] analyzed the variable thermal conductivity effects on three-dimensional Carreau fluid flow over a convectively heated bidirectional sheet subject to modified Fourier law. Recently, Idowu and Falodun [34] observed a decrease in both energy and concentration distributions, while fluid velocity is appreciated to a higher magnitude of thermophysical effects. Idowu et al. [35] established the connection between the Casson fluid and plastic dynamic viscosity boundary layer. Amirsom et al. [36] analyzed the MHD and slip effects over a melting surface with dissipative nanofluid subjected to variable thermo-physical properties. They deduced that a rise in temperature-dependent viscous gave rise to energy distribution but reduces fluid concentration accordingly. Chu et al. [37] investigated the flow past a Riga plate which explains the role of double diffusion in second-grade fluid, therein, variable thermal conductivity, and mass diffusivity upsurge entropy generation and concentration field accordingly. Akolade et al. [38] implement the impacts of variable fluid property in their Soret-Dufour with modified heat flux examination. Sajid et al. [39] investigated the variable diffusivity and thermal conductivity influence on the flow of Maxwell-Sutter by a fluid with activation energy over a stretching surface. While Amani et al. [40] modeled and optimized the viscosity and thermal conductivity effect on the magnetized flow of nanofluid using artificial neural networks. More recently, Ghalambaz et al. [41] and Zadeh et al. [42] investigated the nano-sized capsules flow analysis through the eccentric horizontal cylinder and 2D enclosure respectively where the finite element method was employed to solve the flow analysis of encapsulated phase change material.

Anyakoha [43] and Meyers et al. [44] emphasized on the sensitivity of thermophysical properties, therefore, for an effective estimate of flow processes of heat and mass transfer, it is imperative to account for such variation in any fluid model. Apparently, from the literature analysis and to the knowledge of the authors, little or no study is presented yet on the variable thermophysical effects of squeezing flow as all were based on constant physical properties. As a result, this paper aimed at investigating the influence of variable mass diffusivity, viscosity, and thermal conductivity on MHD, free convective, and unsteady flow of Casson fluid encompassing joule dissipation, radiation influences.

2. Governing systems and problem description

The thermophysical properties namely: mass diffusivity, thermal conductivity and viscosity were assumed variable in the flow problem of an unsteady, two-dimensional incompressible, dissipative, radiating and squeezing flow of MHD conducting Casson fluid through an infinitely parallel plates with metric $h(t) = \pm l(1 - \alpha t)^{1/2}$ apart. The motion is induced as a result of the squeezing property. The lower plate is positioned at $y = 0$ and upper subjected to a metric $h(t)$. The configuration model of the problem is pictured in Fig. 1 with a non-uniform magnetic field $B(x) = B_0(1 - \alpha t)^{1/2}$ of variable strength B_0 imposed perpendicular to the fluid. Joule heating is also considered in this model. At the time t , l denotes the initial plates metric and α represents the characteristic parameter of the squeezing motion of the plate with a dimension of the inverse time.

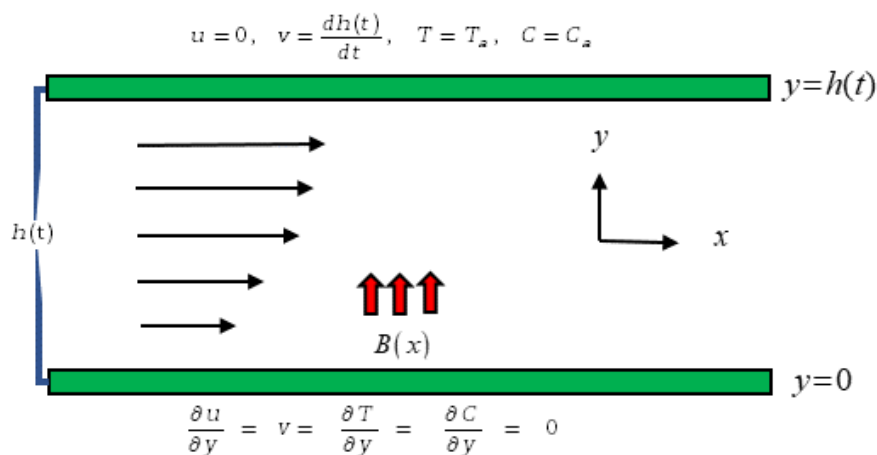


Fig. 1. Model physical coordinate system and configuration



For an isentropic and incompressible Casson fluid, the kinematic viscosity depends on the Casson parameter β , density ρ and temperature dependent plastic dynamic viscosity μ thus given as ([6], [8], [35])

$$\nu = \frac{\mu(T)}{\rho} \left(1 + \frac{1}{\beta} \right), \quad (1)$$

The equations supporting the flow of thermophysical effects in dissipative, chemically radiating and MHD squeezing flow of Casson fluid is presented as thus ([2], [6], [31], [35]);

$$\frac{\partial u}{\partial x} + \frac{\partial v}{\partial y} = 0, \quad (2)$$

$$\frac{\partial u}{\partial t} + u \frac{\partial u}{\partial x} + v \frac{\partial u}{\partial y} = -\frac{1}{\rho} \frac{\partial P}{\partial x} + \frac{1}{\rho} \left(1 + \frac{1}{\beta} \right) \left[\frac{\partial}{\partial x} \left(2\mu(T) \frac{\partial u}{\partial x} \right) + \frac{\partial}{\partial y} \left(\mu(T) \left(\frac{\partial u}{\partial y} + \frac{\partial v}{\partial x} \right) \right) \right] - \frac{\sigma B(x)^2}{\rho(1-\alpha t)} u, \quad (3)$$

$$\frac{\partial v}{\partial t} + u \frac{\partial v}{\partial x} + v \frac{\partial v}{\partial y} = -\frac{1}{\rho} \frac{\partial P}{\partial y} + \frac{1}{\rho} \left(1 + \frac{1}{\beta} \right) \left[\frac{\partial}{\partial y} \left(2\mu(T) \frac{\partial v}{\partial y} \right) + \frac{\partial}{\partial x} \left(\mu(T) \left(\frac{\partial u}{\partial y} + \frac{\partial v}{\partial x} \right) \right) \right], \quad (4)$$

$$\frac{\partial T}{\partial t} + u \frac{\partial T}{\partial x} + v \frac{\partial T}{\partial y} = \frac{1}{\rho C_p} \left[\frac{\partial}{\partial y} \left(\kappa(T) \frac{\partial T}{\partial y} \right) + \frac{\partial}{\partial x} \left(\kappa(T) \frac{\partial T}{\partial x} \right) \right] + \frac{1}{\rho C_p} \frac{16\sigma^* T_0^3}{3k_e} \frac{\partial^2 T}{\partial y^2} + \frac{\sigma B(x)^2}{\rho C_p (1-\alpha t)} u^2 + \frac{\mu(T)}{\rho C_p} \left(1 + \frac{1}{\beta} \right) \left[4 \left(\frac{\partial u}{\partial x} \right)^2 + \frac{\partial v}{\partial x} + \frac{\partial u}{\partial y} \right], \quad (5)$$

$$\frac{\partial C}{\partial t} + u \frac{\partial C}{\partial x} + v \frac{\partial C}{\partial y} = \frac{\partial}{\partial x} \left(D(c) \frac{\partial C}{\partial x} \right) + \frac{\partial}{\partial y} \left(D(c) \frac{\partial C}{\partial y} \right) - \frac{K_r(t)}{(1-\alpha t)} (C - C_0), \quad (6)$$

subjected to

$$\begin{aligned} \frac{\partial u}{\partial y} = v = \frac{\partial T}{\partial y} = \frac{\partial C}{\partial y} = 0 \text{ at } y=0, \\ u=0, \quad v = \frac{dh(t)}{dt}, \quad T = T_a, \quad C = C_a, \text{ at } y=h(t). \end{aligned} \quad (7)$$

The variability in plastic dynamic viscosity, coefficient of heat diffusivity and of mass diffusivity and magnetic field is assumed respectively ([35], [31] and [29])

$$\begin{aligned} \mu(T) &= \mu_0 e^{(-m_1(T-T_0))} & \kappa(T) &= \kappa_0 [1 + m_2(T - T_0)] \\ D(c) &= D_0 [1 + m_3(C - C_0)] & B(x) &= B_0 (1 + \alpha t)^{\frac{1}{2}} \end{aligned} \quad (8)$$

To simplify Eqs. (3) and (4) into a single equation and eliminating the pressure term present, we utilize the continuity Eq. (2) and introduce the vorticity equation $\omega = \partial v / \partial x - \partial u / \partial y$, thus Eqs. (3) and (4) is reduced to (Ahmed et al. [2]);

$$\frac{\partial \omega}{\partial t} + u \frac{\partial \omega}{\partial x} + v \frac{\partial \omega}{\partial y} = \frac{1}{\rho} \left(1 + \frac{1}{\beta} \right) \left[2 \frac{\partial \mu(T)}{\partial x} \frac{\partial \omega}{\partial x} + 2 \frac{\partial \mu(T)}{\partial y} \frac{\partial \omega}{\partial y} + \mu(T) \left(\frac{\partial^2 \omega}{\partial y^2} + \frac{\partial^2 \omega}{\partial x^2} \right) \right] + \left[\left(\frac{\partial^2 \mu(T)}{\partial x^2} - \frac{\partial^2 \mu(T)}{\partial y^2} \right) \left(\frac{\partial v}{\partial x} + \frac{\partial u}{\partial y} \right) \right] + 2 \frac{\partial^2 \mu(T)}{\partial x \partial y} \left(\frac{\partial v}{\partial y} - \frac{\partial u}{\partial x} \right) - \frac{\sigma B(x)^2}{\rho(1-\alpha t)} \frac{\partial u}{\partial y} \quad (9)$$

utilizing Eq. (8) on Eqs. (9), (5), (6), (7) and introducing the following transformations in Eq. (10)

$$u = \frac{\alpha x}{2(1-\alpha t)} F_\eta(\eta), \quad v = -\frac{\alpha l}{2(1-\alpha t)^{\frac{1}{2}}} F(\eta), \quad \omega = -\frac{\alpha x}{2l(1-\alpha t)^{\frac{3}{2}}} F_{\eta,\eta}(\eta), \quad \eta = \frac{y}{l(1-\alpha t)^{\frac{1}{2}}}, \quad \varphi(\eta) = \frac{C - C_0}{C_a - C_0}, \quad \theta(\eta) = \frac{T - T_0}{T_a - T_0}. \quad (10)$$

Equations (5), (6) and (9) together with conditions in Eq. (7) are reduced accordingly to an ordinary non-linear, coupled system of equations;

$$\left(1 + \frac{1}{\beta} \right) e^{-\xi_1 \theta} \left[F_{\eta,4} - \xi_1 \theta_{\eta,\eta} F_{\eta,\eta} + \xi_1^2 \theta_{\eta,\eta}^2 F_{\eta,\eta} - 2 \xi_1 \theta_{\eta,\eta}^2 F_{\eta,3} \right] - \epsilon \left[(3 + F_\eta) F_{\eta,\eta} + (\eta - F) F_{\eta,3} \right] - Ha^2 F_{\eta,\eta} = 0, \quad (11)$$

$$\left[1 + \xi_2 \theta + \frac{4}{3} Nr \theta_{\eta,\eta} + \xi_2 \theta_{\eta,\eta}^2 + Pr \epsilon (F - \eta) \theta_{\eta,\eta} + Ec Pr \left[\left(1 + \frac{1}{\beta} \right) e^{-\xi_1 \theta} (4 \delta^2 F_\eta^2 + F_{\eta,\eta}^2) + Ha^2 F_\eta^2 \right] \right] = 0, \quad (12)$$

$$[1 + \xi_3 \varphi] \varphi_{\eta,\eta} + \xi_3 \varphi_{\eta,\eta}^2 + Sc \epsilon (F - \eta) \varphi_{\eta,\eta} - Sc \lambda \varphi = 0, \quad (13)$$



subjected to

$$\begin{aligned} F_{\eta,\eta} &= 0, \quad F = 0, \quad \theta_\eta = 0, \quad \varphi_\eta = 0, \quad \text{at } \eta = 0, \\ F_\eta &= 0, \quad F = 1, \quad \theta = 1, \quad \varphi = 1, \quad \text{at } \eta = 1, \end{aligned} \quad (14)$$

where

$$\begin{aligned} \xi_1 &= (T_a - T_0)m_1, \quad \xi_2 = (T_a - T_0)m_2, \quad \xi_3 = (C_a - C_0)m_3, \quad Sc = \frac{\nu}{D_0}, \quad \epsilon = \frac{\alpha l^2}{2\nu}, \quad \delta = \frac{l(1-\alpha t)^{\frac{1}{2}}}{x}, \quad Ha^2 = \frac{\sigma B_0^2 l^2}{\mu_0}, \\ Pr &= \frac{\mu_0 C_p}{\kappa_0}, \quad Ec = \frac{\alpha^2 x^2}{4C_p(T_a - T_0)(1-\alpha t)^2}, \quad Nr = \frac{4\sigma^* T_0^3}{\kappa_0 k_e}, \quad \lambda = \frac{K_r l^2}{\nu}. \end{aligned}$$

The physical quantities of interest includes; skin friction coefficient, Nusselt number and Sherwood number defined as,

$$C_f = \frac{\left(1 + \frac{1}{\beta}\right) \mu(T) \left(\frac{\partial u}{\partial y}\right)_{y=h(t)}}{\rho v_m^2} \Rightarrow \frac{l^2}{x^2} R_{ex} C_f = \left(1 + \frac{1}{\beta}\right) e^{-\xi_1 \theta(1)} F''(1) \quad (15)$$

$$Nu_x = -\frac{l\kappa(T) \left(1 + \frac{16\sigma^* T_0^3}{3k_e}\right) \left(\frac{\partial T}{\partial y}\right)_{y=h(t)}}{\kappa(T)(T_a - T_0)} \Rightarrow (1-\alpha t)^{\frac{1}{2}} Nu_x = -\left(1 + \frac{4}{3} Nr\right) [1 + \xi_2 \theta(1)] \theta'(1) \quad (16)$$

$$Sh_x = -\frac{lD(c) \left(\frac{\partial C}{\partial y}\right)_{y=h(t)}}{D(c)(C_a - C_0)} \Rightarrow (1-\alpha t)^{\frac{1}{2}} Sh_x = -[1 + \xi_3 \varphi(1)] \varphi'(1) \quad (17)$$

the local Reynolds number define by $R_{ex} = (1-\alpha t)^{1/2} \alpha l x / 2\nu$.

3. Numerical Solution

The governing ordinary, nonlinear, coupled system of Eqs. (12) – (13) with the associated boundary conditions in Eq. (14) is solved via Chebyshev based Collocation Approach (CCA). The approach requires associating an unknown coefficient to the Chebyshev base functions that will represent the trial solution, implement the trial function on the boundary condition and the governing systems to generate the residue. Hence, utilize the collocation techniques so as to approximate the residual error close to zero. CCA is found accurate, and simple considering its effectiveness, simplicity and rapid convergence in approximating both finite, and semi-infinite domain problems (Idowu et al. [35], Babatin [45], Javed, and Mustafa [46], Mallawi [47]).

3.1 Application of Chebyshev based Collocation

The unknown functions $F(\eta)$, $\theta(\eta)$ and $\varphi(\eta)$ are assumed as the sum of Chebyshev base functions

$$F(\eta) = \sum_{n=0}^N a_n T_n(2\eta - 1), \quad \theta(\eta) = \sum_{n=0}^N b_n T_n(2\eta - 1), \quad \varphi(\eta) = \sum_{n=0}^N c_n T_n(2\eta - 1) \quad (18)$$

where a_n , b_n , and c_n are the constants to be determined and $T_n(2\eta - 1)$ is the shifted Chebyshev base function from $[-1, 1]$ to $[0, 1]$. In order to obtained the values of constants a_n , b_n , and c_n , Eq. (18) is substituted into the boundary conditions in Eq. (14) to have

$$\left[\frac{d^2}{d\eta^2} \sum_{n=0}^N a_n T_n(2\eta - 1)\right]_{\eta=0} = 0, \quad \left[\sum_{n=0}^N a_n T_n(2\eta - 1)\right]_{\eta=0} = 0, \quad \left[\frac{d}{d\eta} \sum_{n=0}^N b_n T_n(2\eta - 1)\right]_{\eta=0} = 0, \quad \left[\frac{d}{d\eta} \sum_{n=0}^N c_n T_n(2\eta - 1)\right]_{\eta=0} = 0 \quad (19)$$

$$\left[\frac{d}{d\eta} \sum_{n=0}^N a_n T_n(2\eta - 1)\right]_{\eta=1} = 0, \quad \left[\sum_{n=0}^N a_n T_n(2\eta - 1)\right]_{\eta=1} = 1, \quad \left[\sum_{n=0}^N b_n T_n(2\eta - 1)\right]_{\eta=1} = 1, \quad \left[\sum_{n=0}^N c_n T_n(2\eta - 1)\right]_{\eta=1} = 1 \quad (20)$$

Also, by substituting Eqs. (18) into Eqs. (11) - (13), residues $R_F(\eta, a_n, b_n)$, $R_\theta(\eta, a_n, b_n)$ and $R_\varphi(\eta, a_n, c_n)$ are derived. The residues are minimized as small as possible using collocation techniques as follows

$$\text{For } \delta(\eta - \eta_j) = \begin{cases} 1, & \eta = \eta_j \\ 0, & \text{otherwise} \end{cases}$$

$$\int_0^L R_F(\eta, a_n, b_n) d\eta = R_F(\eta, a_n, b_n) = 0, \quad \text{for } j = 1, 2, \dots, N-3 \quad (21)$$

$$\int_0^L R_\theta(\eta, a_n, b_n) d\eta = R_\theta(\eta, a_n, b_n) = 0, \quad \text{for } j = 1, 2, \dots, N-1 \quad (22)$$



Table 1. Validation of Chebyshev Collocation Method (CCM) results with the results of Mustafa et al. [2] for:
 $Ec = 1, Sc = 1, \delta = 0.1, \lambda = 1, Pr = 1, \xi_2 = Ha = \xi_1 = \xi_3 = \beta = Nr = 0$

	$-F_{\eta\eta}(0)$		$-\theta_{\eta}(0)$		$-\varphi_{\eta}(0)$	
ϵ	Present	Mustafa et al. [2]	Present	Mustafa et al. [2]	Present	Mustafa et al. [2]
-1.0	2.170090	2.1700908	3.319899	3.3198992	0.804558	0.8045587
-0.5	2.614038	2.61740384	3.129491	3.1294910	0.7814023	0.78140234
0.01	3.007134	3.0071337	3.047092	3.0470919	0.7612252	0.76122521
0.5	3.336449	3.3364494	3.026324	3.0263235	0.7442243	0.74422428
2.0	4.167389	4.1673891	3.118551	3.1185506	0.7018132	0.70181323

$$\int_0^1 R_{\varphi}(\eta, a_n, c_n) d\eta = R_{\varphi}(\eta, a_n, c_n) = 0, \quad \text{for } j = 1, 2, \dots, N-1, \quad (23)$$

where η_j is the shifted Gauss lobatto collocation points defined as

$$\eta_j = \frac{1}{2} \left(1 - \cos \left(\frac{j\pi}{N} \right) \right), \quad \text{for } j = 0, 1, \dots, N. \quad (24)$$

In this manner, Eqs. (19 -23) form a system of $3N+3$ algebraic equations with $3N+3$ unknown coefficients a_n, b_n , and c_n are obtained. The obtained system of equations is solved using Newton method. All the computation in this work are carried out with the help of Mathematical symbolic package MATHEMATICA 11.3. The square residual error for $F(\eta)$, $\theta(\eta)$ and $\varphi(\eta)$ are computed as presented in Eq. (25) and the graph of total average square residual error ($\epsilon_{total} = (\epsilon_F + \epsilon_{\theta} + \epsilon_{\varphi}) / 3$) is displayed in Fig. 2. It is observed that the total average square residual error reduces as the value of n is increased.

$$\epsilon_F = \int_0^1 R_F^2(\eta) d\eta, \quad \epsilon_{\theta} = \int_0^1 R_{\theta}^2(\eta) d\eta, \quad \epsilon_{\varphi} = \int_0^1 R_{\varphi}^2(\eta) d\eta \quad (25)$$

In order to check for the accuracy of the used method, the obtained results are compared with that of Mustafa et al. [2], and a good agreement is found

4. Result and Discussion

The results of velocities, energy, concentration, Skin friction, Nusset number and Sherwood number are obtained and computed for the fixed values of $\xi_1 = \xi_2 = \xi_3 = 0.1$, $\beta = 0.2$, $Nr = 0.1$, $\delta = 0.5$, $Sc = 0.7$, $\lambda = 0.1$, $Ec = 0.1$, $Pr = 1$, $Ha = 0.5$, $\epsilon = 0.5$ throughout the investigation else otherwise stated, thus Fig. 2-10 present the graphical results of the influence of pertinent parameters on the flow field. In order to test for the accuracy of the used method, the obtained results for skin friction, Nuselt number and Sherwood number are compared with the results of Mustafa et al. [2] and Al-Saif and Harfash,. [20], thus, a good agreement is found as it is shown in Table 1 and 2.

Figure 3 displayed the influence of variable viscosity (ξ_1) and squeezing (ϵ) parameters on the dimensionless normal $F(\eta)$ and radial $F_{\eta}(\eta)$ velocities. Viscosity being an important (determinant) flow characteristic of any non-Newtonian fluid, among which Casson fluid is of no exception, with shear thinning behavior. Physically, good enhancement of fluid viscosity results to fluid flow velocities resistivity. Hence resulted to reduction in fluid velocities as perceived on Fig. 3. Obviously seen in Fig. 3b the radial velocity $F_{\eta}(\eta)$ appreciates along the moving plate but depreciate on the lover plate. Squeezing effect likewise displayed a reduction pattern on velocity profiles for both negative and positive ϵ . Knowing that a rise in squeeze parameter deforms the fluid property, thus the radial velocity is seen appreciable within the flow region $\eta > 0.5$.

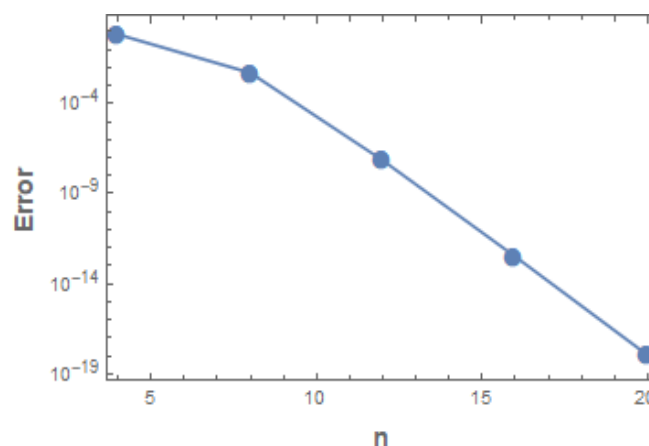


Fig. 2. Minimized residual error



Table 2. Validation of Chebyshev Collocation Method (CCM) results with the work of Al-Saif and Harfash, [20] for varying η at $Ec = 0.5, \varepsilon = 0.5, Sc = 1, \delta = 0.1, \lambda = 1, Pr = 2, \xi_2 = Ha = \xi_1 = \xi_3 = \beta = Nr = 0$

η	$F(\eta)$		$\theta(\eta)$		$\varphi(\eta)$	
	Present	Al-Saif, and Harfash [20]	Present	Al-Saif, and Harfash [20]	Present	Al-Saif, and Harfash [20]
0	0	0	1.6841811265	1.6853846217	0.7952078482	0.7930840909
0.1	0.1453846919	0.1453798050	1.6837054338	1.6849083511	0.7971963182	0.7950970401
0.2	0.2882598533	0.2882508397	1.6816666187	1.6828642524	0.8031671989	0.8011410434
0.3	0.4260659649	0.4260542054	1.6761885934	1.6773661830	0.8131374065	0.8112320454
0.4	0.5561433939	0.5561306350	1.6640033631	1.6651314686	0.8271368359	0.8253982358
0.5	0.6756820190	0.6756700441	1.6402214098	1.6412547142	0.8452109893	0.8436825495
0.6	0.78167054549	0.7816608303	1.5979721550	1.5988535623	0.8674248191	0.8661463397
0.7	0.8708455258	0.8708389416	1.5278701919	1.5285420825	0.8938679679	0.8928744148
0.8	0.9396402218	0.9396368409	1.4172394643	1.4176628081	0.9246616732	0.9239817330
0.9	0.9841336037	0.9841326623	1.24899186775	1.2491703840	0.9599677220	0.9596221744
1.0	1	1	1	1	1	1

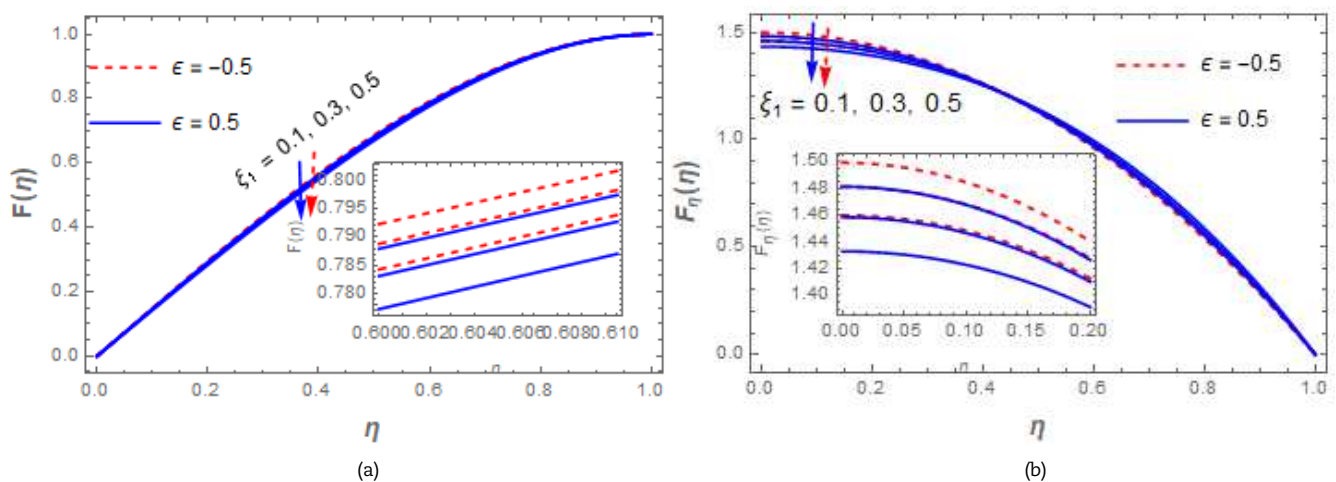


Fig. 3. Behavior of ξ_1 and ε on (a) normal $F(\eta)$ and (b) radial $F_\eta(\eta)$ velocities

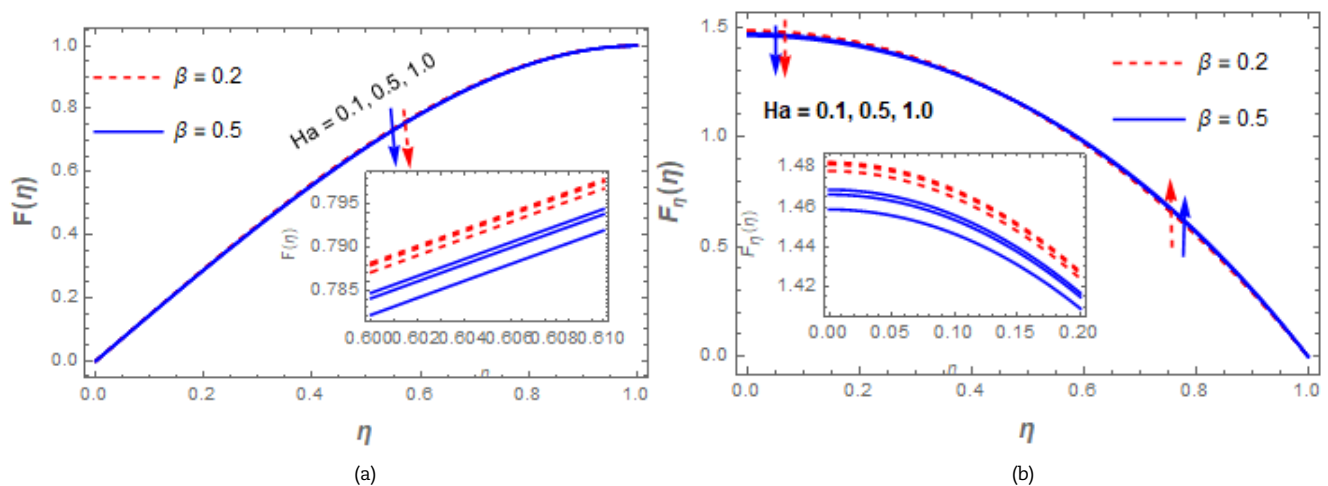
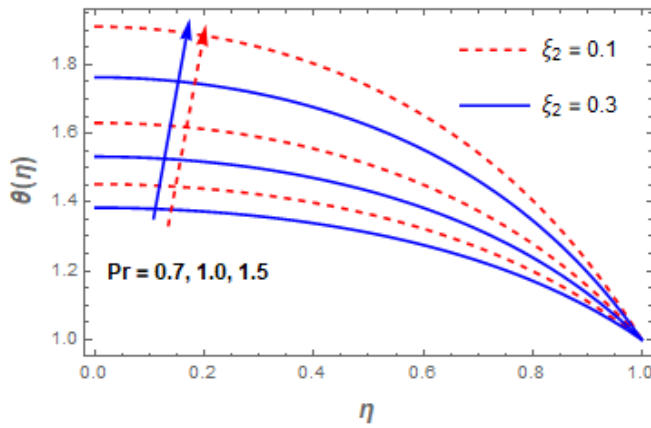
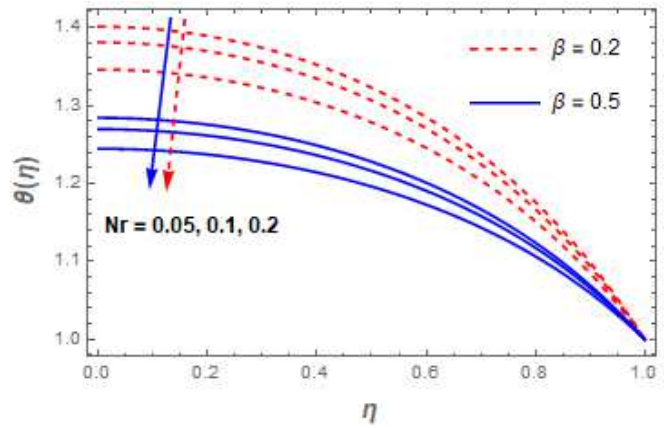
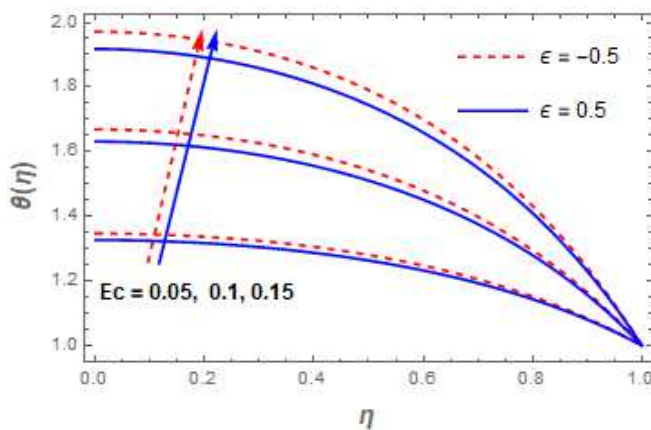
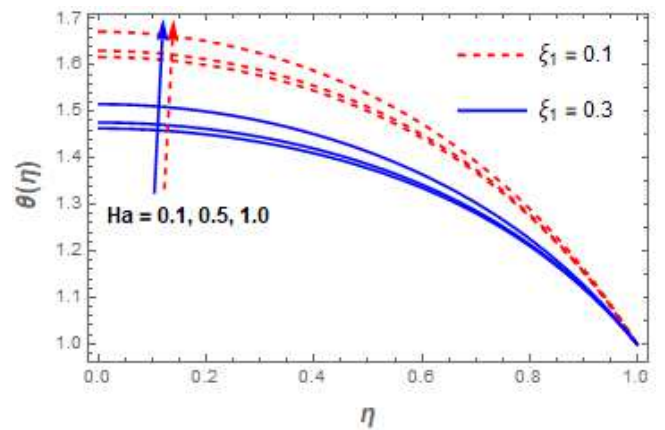


Fig. 4. Behavior of Ha and β on (a) normal $F(\eta)$ and (b) radial $F_\eta(\eta)$ velocities

Figure 4 depicts the influence of Hartmann number (Ha) and Casson (β) parameter on the dimensionless (a) normal $F(\eta)$ and (b) radial $F_\eta(\eta)$ velocities. The present investigation proved that continuous injection of β into the flow system nullifies the present model to Newtonian category. The characterization of β within the flow region obeys the law of viscosity (i.e. $\beta \rightarrow \infty$). An appreciation in β produce a reduction in yield stress, thus a decline behavior of both normal and radial velocities was experienced. A rise in Hartmann number (Ha) signifies an enhancement of the transverse magnetic field which magnified the resistivity (Lorentz) force, thereby reducing the magnitude of both normal and axial squeezing flow velocities.



Fig. 5. Behavior of Pr and ξ_2 on $\theta(\eta)$ Fig. 6. Behavior of Nr and β on $\theta(\eta)$ Fig. 7. Behavior of Ec and ϵ on $\theta(\eta)$ Fig. 8. Behavior of Ha and ξ_1 on $\theta(\eta)$

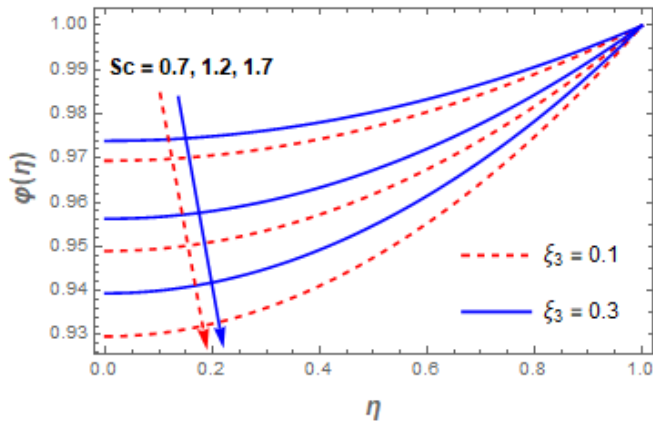
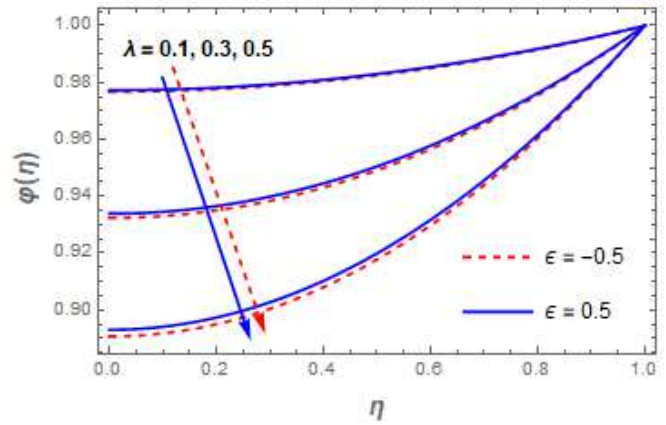
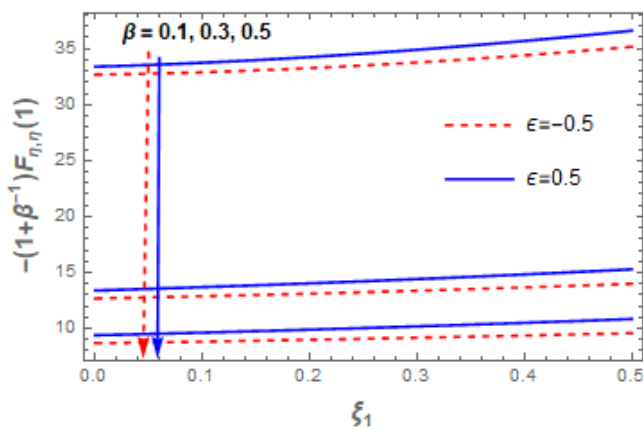
Variability of thermal conductivity and Prandtl number is accounted for in Fig. 5. The random movement of molecular motion (thermal conductive property), (ξ_2), across the squeezing channel presents a destructive influence to the thermal field and seen conserving the heat generated by the fluid, thus rise in ξ_2 enhances the temperature field. Hence, liberating ξ_2 may be attributed to weakening bound of Casson fluid as a result of temperature difference. Physically, during heat transfer analysis, accelerated thermal field is attributed to lessen in thermal conductivity values. Thus, temperature profiles are appreciated to a hike in mass diffusion to thermal diffusion ratio (Pr).

Figure 6 portrays the rheological representation of blood (Casson fluid) parameter (β) and Radiation (Nr) influence on energy profile. Radiation acts as a heat source within the fluid region, however, in energy equation (5), thermal relation is seen lessening the mean absorption coefficient, thus a hike in radiation dosage decreases the fluid temperature. Similarly, an appreciable value of β decelerates the energy distribution significantly throughout the entire flow medium. Dissipation (Ec) and squeezing (ϵ) effects on temperature field are presented in Fig. 7. In this flow process, an improvement in heat generation is perceived due to higher friction force between the fluid particles arising from higher magnitude of Ec . Thus, collision between the fluid molecules increases and the fluid energy improved significantly. Contrarily, the plate movement parameter (squeezing number) demonstrated a downsize behavior on the energy field, as a result of decaying squeeze force to higher squeezing number.

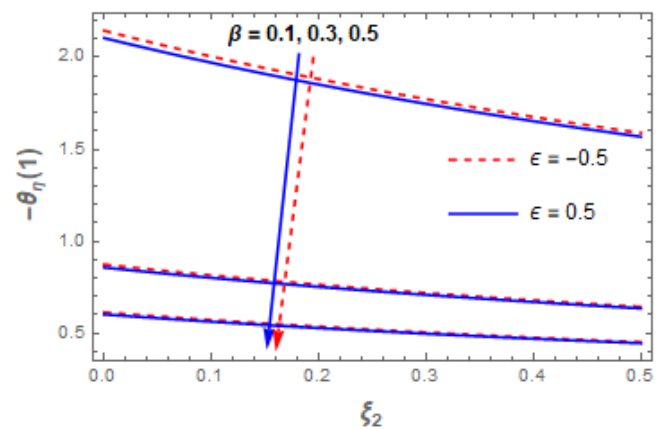
Figure 8 demonstrates the uplifting values of Hartmann number and variable viscosity on energy distribution. Growing value of Hartmann number accelerate the fluid temperature throughout the flow domain while the viscosity effect is seen lessen the fluid thermal profiles. Response in Casson fluid concentration with a variation in both variable diffusivity parameter, ξ_3 , and Schmidt number, Sc , is presented in Fig. 9. Variability of ξ_3 obviously portray a higher profile against concentration field. The purpose behind this phenomenon tells that an enhancement in mass diffusivity parameter is required to account for further mass transfer. It is worth mentioning that concentration field decreases with a rise in Sc number, but a higher magnitude of ξ_3 indicate that concentration field increases with a positive effect of Sc .

Figure 10 account for the variation of squeezing and chemical reaction parameters on concentration field. Generally, positive reaction parameter retards the flow concentration and accelerates to a decreasing value. Meanwhile, an appreciable value of λ decelerate the concentration of the squeezing fluid as depicted. Physically, to-and-fro motion of the plates create an intermolecular force within the Casson fluid particles which in turn accelerate the fluid concentration. Thus, rise in squeeze parameter (ϵ) appreciate the fluid concentration.

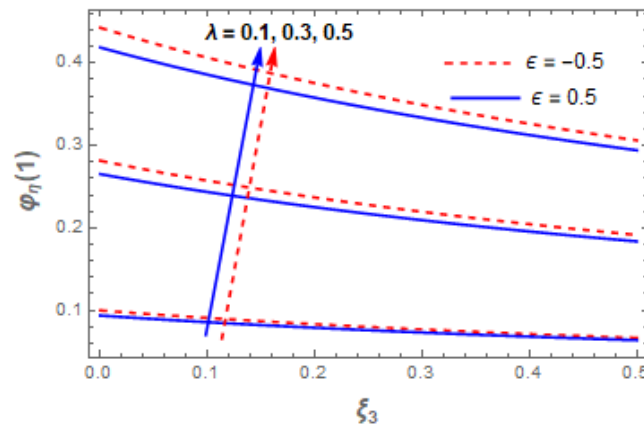


Fig. 9. Behavior of Sc and ξ_3 on $\theta(\eta)$ Fig. 10. Behavior of λ and ϵ on $\theta(\eta)$ 

(a)



(b)



(c)

Fig. 11. Influence of flow physical characteristics (a) Skin friction, (b) Nusselt number and (c) Sherwood number.

The influence of squeezing, Casson and viscosity parameter on Skin friction coefficient is presented in Figs. 11, clearly β is seen decreasing the skin friction coefficient and appreciate to an increasing values of ξ_1 and ϵ . ξ_3 , β and ϵ decreases the Heat transfer coefficient, while ξ_3 and ϵ downsized off the rate of mass transfer.

5. Conclusion

An investigation into thermophysical properties of chemically reacting Squeezed flow of Dissipative Casson fluid encompassing the radiation, MHD effects is studied. The governing equations assisting the flow is formulated and transformed using a suitable similarity transformation. Hence, the solution to the resulting sets of ODEs dimensionless model is approximated numerically via Chebyshev based Collocation Approach (CCA). The solution technique gave an excellent approximation as seen in Table 1. Thus, the following conclusions were drawn:



1. The concentration field is appreciated to a higher magnitude of ξ_3 and ϵ parameters, while velocities and temperature depreciate with an increasing function of ξ_1 , ξ_2 and ϵ accordingly,
2. Velocities and energy fields is downsized to a large value of Ha and β ,
3. Higher numbers of Ec and Pr appreciate the temperature field rapidly,
4. Chemical reaction decreases the concentration field,
5. Increasing values of radiation parameter lessen the temperature field,
6. Skin friction, Heat and Mass transfer coefficients diminished to a rise in variable thermal and mass diffusivity parameter while variable viscosity pronounced the skin friction coefficient.

Interestingly, present analysis is helpful in optimizing and modeling of viscosity, mass diffusivity and thermal conductivity rate of fluid materials in a given system. Future work will involve introduction of nanofluids to enhance the optimality of heat transfer conditions and consider squeeze flow in more fluid type and complex geometries.

Author Contributions

M.T. Akolade and J.O. Olabode initiated the project, A.T. Adeosun, J.O. Olabode and M.T. Akolade carried out the mathematical modeling and examined the theory validation. M.T. Akolade introduced and transformed the governing problem, J.O. Olabode and M.T. Akolade presented the literature survey, A.T. Adeosun planned the numerical scheme and presented the numerical computations. The manuscript was written through the contribution of all authors. All authors discussed the results, and approved the reviewed version of the manuscript.

Conflict of Interest

The authors declared no potential conflicts of interest with respect to the research, authorship and publication of this article.

Funding

The authors received no financial support for the research, authorship and publication of this article.

Nomenclature

B_0	Magnetic field [Weber/m ²]	m_1	variation of viscosity [kg/ms]
C	Fluid concentration [mol.]	m_2	variation of thermal conductivity [W/mK]
C_a	Wall surface concentration [mol.]	m_3	variation of mass diffusivity [kg/m ² /s]
C_p	Specific heat capacity [J/kg.K]	Nr	Radiation parameter [-]
D_0	Mass diffusivity [kg/m ² /s]	P	pressure gradient [N·m ⁻²]
Ec	Eckert number [-]	Pr	Prandtl number [-]
F	Dimensionless velocity [-]	Sc	Schmidt number [-]
Ha	Magnetic parameter [-]	t	Time [s]
K_e	Absorption coefficient [m ⁻¹]	T	Fluid temperature [K]
K_r	Dimensional chemical reaction parameter [-]	T_a	Wall surface temperature [K]
k_0	Thermal conductivity [W/mK]	T_0	Reference temperature [K]
l	Initial plate distance [L]	u, v	Velocities along x and y direction [m/s]

Greek Symbols

α	Squeezing characteristics parameter [L]	ν	Kinematic viscosity [kg m ⁻¹ s ⁻¹]
β	Casson parameter	ξ_1	dimensionless viscosity [-]
δ	Fluid Dimensionless number [-]	ξ_2	dimensionless thermal conductivity [-]
ϵ	Squeezing parameter [-]	ξ_3	dimensionless mass diffusivity [-]
η	Dimensionless plate length [L]	ρ	Fluid density [kg/m ³]
θ	Dimensionless Temperature [-]	σ	Electric conductivity [S/m]
λ	Dimensionless chemical reaction parameter [-]	σ^*	Stefan-Boltzmann constant [W m ² K ⁻⁴]
μ_0	Dynamic viscosity [kg m ⁻¹ s ⁻¹]	φ	Dimensionless Concentration [-]

References


- [1] Stefan, M.J., Versuch uber die scheinbare adhesion, Sitzungsber Sachs Akad Wiss Wein, *Math. Nat. Wiss.*, 69, 1874, 713-721.
- [2] Mustafa, M., Hayat, T., Obaidat, S., On heat and mass transfer in the unsteady squeezing flow between parallel plates, *Meccanica*, 47, 2012, 1581-1589.
- [3] Khan, H., Qayyum, M., Khan, O., Ali, M., Unsteady Squeezing Flow of Casson Fluid with Magnetohydrodynamic Effect and Passing through Porous Medium, *Mathematical Problems in Engineering*, 2016, Article ID 4293721.
- [4] Ahmed, N., Khan, U., Khan, S., Bano, S., Mohyud-Din, S., Effects on magnetic field in squeezing flow of a Casson fluid between parallel plates, *Journal of King Saud University-Science*, 29, 2017, 119-125.
- [5] Qayyum, M., Khan, H., Khan, O., Slip Analysis at Fluid-Solid Interface in MHD Squeezing Flow of Casson Fluid through Porous Medium, *Results in Physics*, 7, 2017, 732-750.
- [6] Naduvnamani, N., Shankar, U., Radiative squeezing flow of unsteady magneto-hydrodynamic Casson fluid between two parallel plates, *Journal of Central South University*, 26(5), 2019, 1184-1204.
- [7] Singh, K., Rawat, S., Kumar, M., Heat and Mass Transfer on Squeezing Unsteady MHD Nanofluid Flow between Parallel Plates with Slip Velocity Effect, *Journal of Nanoscience*, 2016, Article ID 9708562.
- [8] Ghadikolaei, S.S., Hosseinzadeh, K., Ganji, D.D., Analysis of unsteady MHD Eyring-Powell squeezing flow in stretching channel with considering thermal radiation and Joule heating effect using AGM, *Case Studies in Thermal Engineering*, 10, 2017, 579-594.
- [9] Hussain, A., Akbar, S., Sarwar, L., Malik, M. Y., Numerical investigation of squeezing flow of Walter's-B fluid through parallel plates, *Journal of the Brazilian Society of Mechanical Sciences and Engineering*, 41, 2019, 477-483.
- [10] Ahmad, S., Farooq, M., Javed, M., Anjum, A., Slip analysis of squeezing flow using doubly stratified fluid, *Results in Physics*, 9, 2018, 527-533.
- [11] Ahmad, S., Farooq, M., Anjum, A., Mir, N.A., Squeezing flow of convectively heated fluid in porous medium with binary chemical reaction and





activation energy, *Advances in Mechanical Engineering*, 11(10), 2019, 1-12.

- [12] Hosseinzadeh, Kh., Alizadeh, M., Ganji, D.D., Hydrothermal analysis on MHD squeezing nanofluid flow in parallel plates by analytical method, *International Journal of Mechanical and Materials Engineering*, 13(4), 2018, 1-12.
- [13] Thumma, T., Magagula, V.M., Transient electromagnetohydrodynamic radiative squeezing flow between two parallel Riga plates using a spectral local linearization approach, *Heat Transfer*, 49, 2020, 67-85.
- [14] Salehi, S., Nori, A., Hosseinzadeh, Kh., Ganji, D.D., Hydrothermal analysis of MHD squeezing mixture fluid suspended by hybrid nanoparticles between two parallel plates, *Case Studies in Thermal Engineering*, 21, 2020, DOI: 10.1016/j.csite.2020.100650.
- [15] Zhao, C., Zhang, W., Van Den Ende, D., Mugele, F., Electroviscous effects on the squeezing flow of thin electrolyte solution films, *Journal of Fluid Mechanics*, 888, 2020, A29-A36.
- [16] Khan, S.I.U., Alzahrani, E., Khan, U., Zeb, N., Zeb, A., On Mixed Convection Squeezing Flow of Nanofluids, *Energies*, 13, 2020, 3138-3156.
- [17] Ahmad, S., Farooq, M., Rizwan, M., Ahmad, B., Rehman, S.U., Melting Phenomenon in a Squeezed Rheology of Reactive Rate Type Fluid, *Frontiers in Physics*, 8, 2020, Article 108.
- [18] Qayyum M., Khan O., Abdeljawad T., Imran N., Sohail M., Al-Kouz W., On Behavioral Response of 3D Squeezing Flow of Nanofluids in a Rotating Channel, *Complexity*, 2020, 1-16, Article ID 8680916.
- [19] Korczyk, P. M., Steijn V. V., Blonski S., Zaremba D., Beattie D. A., Garstecki P., Accounting for corner flow unifies the understanding of droplet formation in microfluidic channels, *Nature Communications*, 10, 2019, 2528.
- [20] Al-Saif, A.S.J., Harfash, A.J., Perturbation-Iteration Algorithm for Solving Heat and Mass Transfer in the Unsteady Squeezing Flow between Parallel Plates, *Journal of Applied Computational Mechanics*, 5(4), 2019, 804-815.
- [21] Animasaun, I.L., Effects of thermophoresis, variable viscosity and thermal conductivity on free convective heat and mass transfer of non-darcian MHD dissipative Casson fluid flow with suction and nth order of chemical reaction, *Journal of the Nigerian Mathematical Society*, 34, 2015, 11-31.
- [22] Barcroft, H., Edholm, O.G., The effect of temperature on blood flow and deep temperature in the human forearm, *Journal of Physiology*, 102, 1943, 5-20.
- [23] Khan, W., Gul, T., Idrees, M., Islam, S., Khan, I., Dennis, L.C.C., Thin Film Williamson Nanofluid Flow with Varying Viscosity and Thermal Conductivity on a Time-Dependent Stretching Sheet, *Applied Science*, 6, 2016, 334-356.
- [24] Basha, H.T., Sivaraj, R., Reddy, A.S., Chamkha, A.J., Tilioua, M., Impacts of temperature-dependent viscosity and variable Prandtl number on forced convective Falkner-Skan flow of Williamson nanofluid, *SN Applied Sciences*, 2, 2020, 477-490.
- [25] Waqas, M., Alsaedi, A.S., Shehzad, A., Hayat, T., Asghar, S., Mixed convective stagnation point flow of Carreau fluid with variable properties, *Journal of the Brazilian Society of Mechanical Sciences and Engineering*, 39, 2017, 3005-3017.
- [26] Abdul-Wahab, H., Zeb, H., Bhatti, S., Gulistan, M., Kadry, S., Nam, Y., Numerical Study for the Effects of Temperature Dependent Viscosity Flow of Non-Newtonian Fluid with Double Stratification, *Applied Science*, 10, 2020, 708-728.
- [27] Omowaye A.J., Animasaun, I.L., Upper-Convected Maxwell fluid flow with variable Thermo-Physical properties over a melting surface situated in hot environment subject to thermal stratification, *Journal Applied Fluid Mechanics*, 9(4), 2016, 1777-1790.
- [28] Mondal, R.K., Reza-E-Rabbi, S., Gharami, P.P., Ahmmed, S.F., Arifuzzaman, S.M., A Simulation of Casson Fluid Flow with Variable Viscosity and Thermal Conductivity Effects, *Mathematical Modelling of Engineering Problems*, 6(4), 2019, 625-633.
- [29] Salahuddin, T., Arshad, M., Siddique, N., Alqahtani, A.S., Malik, M.Y., Thermophysical properties and internal energy change in Casson fluid flow along with activation energy, *Ain Shams Engineering Journal*, 2020, DOI: 10.1016/j.asej.2020.02.011.
- [30] Idowu, A.S., Falodun, B.O., Variable thermal conductivity and viscosity effects on non-Newtonian fluids flow through a vertical porous plate under Soret-Dufour influence, *Mathematics and Computers in Simulation*, 177, 2020, 358-384.
- [31] Gbadeyan, J.A., Titiloye, E. O., Adeosun, A.T., Effect of variable thermal conductivity and viscosity on Casson nanofluid flow with convective heating and velocity slip, *Heliyon*, 6, 2020, 03076.
- [32] Hazarika, G.C., Phukan, B., Ahmed, S., Effect of variable viscosity and thermal conductivity on unsteady free convective flow of a micropolar fluid past a vertical cone, *Journal of Engineering Physics and Thermophysics*, 93(1), 2020, 184-191.
- [33] Lu, D., Mohammad, M., Ramzan, M., Bilal, M., Howari, F., Suleman, M., MHD Boundary Layer Flow of Carreau Fluid over a Convectively Heated Bidirectional Sheet with Non-Fourier Heat Flux and Variable Thermal Conductivity, *Symmetry*, 11, 2019, 618-631.
- [34] Idowu, A.S., Falodun, B.O., Effects of thermophoresis, Soret-Dufour on heat and mass transfer flow of magnetohydrodynamics non-Newtonian nanofluid over an inclined plate, *Arab Journal of Basic and Applied Sciences*, 27(1), 2020, 149-165.
- [35] Idowu, A.S., Akolade, M.T., Abubakar, J.U., Falodun, B.O., MHD free convective heat and mass transfer flow of dissipative Casson fluid with variable viscosity and thermal conductivity effects, *Journal of Taibah University for Science*, 14(1), 2020, 851-862.
- [36] Amirsom, N.A., Uddin, M.J., Md Basir, M.F., Kadir, A., Beg, O.A., Md. Ismail, A.I., Computation of Melting Dissipative Magnetohydrodynamic Nanofluid Bioconvection with Second-order Slip and Variable Thermophysical Properties, *Applied Science*, 9, 2019, 2493-2511.
- [37] Chu Y., Shah F., Khan M.I., Kadry S., Abdelmalek Z., Kha W.A., Cattaneo-Christov double diffusions (CCDD) in entropy optimized magnetized second grade nanofluid with variable thermal conductivity and mass diffusivity, *Journal of Materials Research and Technology*, 9, 2020, 13977-13987.
- [38] Akolade M.T., Idowu A.S., Adeosun A.T., Multislip and Soret-Dufour influence on nonlinear convection flow of MHD dissipative casson fluid over a slendering stretching sheet with generalized heat flux phenomenon, *Heat Transfer*, 2021, 1-21, <https://doi.org/10.1002/htj.22057>.
- [39] Sajid T., Tanveer S., Sabir Z., Guirao J.L.G., Impact of Activation Energy and Temperature-Dependent Heat Source/Sink on Maxwell-Sutterby Fluid, *Mathematical Problems in Engineering*, 2020, DOI: 10.1155/2020/5251804.
- [40] Amani, M., Amani, P., Kasaeian, A., Mahian, O., Pop, I., Wongwises, S., Modeling and optimization of thermal conductivity and viscosity of MnFe2O4 nanofluid under magnetic field using an ANN, *Scientific Reports*, 7, 2017, 17369.
- [41] Ghalambaz, M., Mehryan, S.A.M., Mozaffari, M., Zadeh, S.M.H., Pour, M.S., Study of thermal and hydrodynamic characteristics of water-nano-encapsulated phase change particles suspension in an annulus of a porous eccentric horizontal cylinder, *International Journal of Heat and Mass Transfer*, 156, 2020, 119792.
- [42] Zadeh, S.M.H., Mehryan, S.A.M., Islam, M.S., Ghalambaz, M., Irreversibility analysis of thermally driven flow of a water-based suspension with dispersed nano-sized capsules of phase change material, *International Journal of Heat and Mass Transfer* 155, 2020, 119796.
- [43] Anyakoha, M.W., *New School Physics*, 3rd Edition, Africana First Publisher Plc, 2010.
- [44] Meyers, T.G., Charpin, J.P.F., Tshela, M.S., The flow of a variable viscosity fluid between parallel plates with shear heating, *Applied Mathematics Model*, 30(9), 2006, 799-815.
- [45] Babatin M.M., Numerical treatment for the flow of Casson fluid and heat transfer model over an unsteady stretching surface in the presence of internal heat generation/absorption and thermal radiation, *Applications & Applied Mathematics*, 13(2), 2018, 854-862.
- [46] Javed, T., Mustafa, I., Slip effect on a mixed convection flow of a third-grade fluid near the orthogonal stagnation point on a vertical surface, *Journal of Applied Mechanics and Technical Physics*, 57(3), 2016, 527-536.
- [47] Mallawi, F., Application of a legendre collocation method to the space time variable fractional-order advection dispersion equation, *J. Taibah Univ. Sci.*, 13(1), 2019, 324-330.

ORCID iD

Mojeed T. Akolade  <https://orcid.org/0000-0002-6876-7203>

Adeshina T. Adeosun  <https://orcid.org/0000-0001-5556-9593>

John O. Olabode  <https://orcid.org/0000-0002-7858-3088>



© 2021 Shahid Chamran University of Ahvaz, Ahvaz, Iran. This article is an open access article distributed under the terms and conditions of the Creative Commons Attribution-NonCommercial 4.0 International (CC BY-NC 4.0 license) (<http://creativecommons.org/licenses/by-nc/4.0/>).



How to cite this article: Akolade M.T., Adeosun A.T., Olabode J.O. Influence of Thermophysical Features on MHD Squeezed Flow of Dissipative Casson Fluid with Chemical and Radiative Effects, *J. Appl. Comput. Mech.*, 7(4), 2021, 1999–2009.
<https://doi.org/10.22055/JACM.2020.34909.2508>

Publisher's Note Shahid Chamran University of Ahvaz remains neutral with regard to jurisdictional claims in published maps and institutional affiliations.

